Eur. Phys. J. D **32**, 63–68 (2005)
DOI: 10.1140/epjd/e2004-00184-1

THE EUROPEAN PHYSICAL JOURNAL D

Self-defocusing/focusing of a relativistic laser pulse in a multiple-ionizing gas

Naveen Kumar[a], V.K. Tripathi, and B.K. Sawhney

Department of Physics, Indian Institute of Technology, 110016 New Delhi, India

Received 4 June 2004 / Received in final form 7 September 2004
Published online 14 December 2004 –

Abstract. A fast rising flattop high power laser pulse, with Gaussian intensity distribution along its wavefront, causes single and double ionizations of the gas through which it propagates. The foot of the pulse causes single ionization of the gas and creates a sharp radial density profile resulting in strong defocusing of the front part of the pulse. After a little while, single state ionization saturates, creating a flat density profile in the axial region and weakening the divergence of the pulse. As the intensity of the pulse rises further, second state ionization occurs, causing strong defocusing of the beam. Later in time when the second state ionization saturates, the relativistic mass nonlinearity together with the electron cavitation tends to focus the pulse.

PACS. 52.38.Hb Self-focussing, channeling, and filamentation in plasmas – 42.65.Jx Beam trapping, self-focusing and defocusing; self-phase modulation

1 Introduction

With the recent advancements in laser technology, laser systems producing pulses of multi-terawatt power have become common. These pulses when focused to a micron spot size with adaptive optics can produce intensities as high as $\approx 10^{21}$ W/cm^2 [1]. The interaction of such a high power laser pulse with gases and plasmas is a major field of research because of its application in laser driven fusion, laser electron accelerator, X-ray lasers, super-continuum generation, and proton acceleration [2–13]. For many of these applications, it is required that the laser pulse propagates over many Rayleigh lengths without considerable energy loss and significant diffraction.

A laser pulse, with an intensity $\geq 10^{15}$ W/cm^2, passing through a gaseous medium can ionize the gas by tunnel ionization [14,15]. The electric field of the pulse provides sufficient velocity to electrons to surpass the coulomb barrier of the nucleus and ionize the gas. As the laser intensity increases, multiple ionizations also occur and the gas becomes fully ionized. However, ionization induced diffraction diverges the laser pulse significantly and restricts the further ionization of the gas. When the power of the pulse exceeds the critical power for relativistic self-focusing, $P_c = 17\,(\omega/\omega_p)^2$ GW, where ω is the carrier frequency of the laser pulse and $\omega_p^2 = 4\pi e^2 n_0/m$ is the plasma frequency of the medium (m is the electron mass, n_0 is the plasma electron density), the laser pulse can be relativistically self-focused [16]. However, tunnel ionization can defocus the light and increase the self-focusing threshold by increasing the on-axis density and refractive index. The laser pulse also exerts a ponderomotive force on the electrons, pushing them away from the propagation axis of the laser pulse, thereby creating an electron-depleted region. This process is known as electron cavitation and assists the process of relativistic self-focusing. The first experimental observation of relativistic self-focusing was made by Borisov et al. [17]. They employed a 0.5-ps 0.3-TW pulse at $\lambda_0 = 0.25$ μm focused into a 7-μm diameter focal spot inside a gas cell; the maximum irradiance was 8×10^{17} W/cm^2. They observed a channel of radius <1 μm and a peak intensity of $\sim 10^{19}$ W/cm^2. They compared their experimental data with theoretical results and found excellent agreement.

Recently, numerous experiments have been performed on helium as well as on other gases [18–20]. Chessa et al. [18] have reported experimental results on intense short pulse laser interaction with helium gas. They employed 1.8-ps, terawatt pulses focused to an intensity of 6×10^{17} W/cm^2. At this intensity, helium gas is doubly ionized. They observed different amounts of blue shift of the laser pulse at different gas pressures. They also observed a more than five times increase in beam spot size for propagation over four Rayleigh lengths. Fedosejevs et al. [19] have reported experiments on many gases including helium, hydrogen, nitrogen etc. They employed a 0.3-TW, 250-fs laser pulse, focused to an intensity of 3×10^{17} W/cm^2. They observed the relativistic self-focusing for hydrogen gas. Sarkisov et al. [20] have reported results on the dynamics of the interaction of a 4-TW, 400-fs pulse

[a] e-mail: naveenpoincare@rediffmail.com

of intensity 6×10^{18} W/cm^2 with a He gas jet. They observed relativistic self-focusing, channel formation, and high-energy ion generation.

Essarey et al. [21] have given an extensive review of the self-focusing and the self-guiding of short laser pulses in ionizing gases and plasmas within the framework of the near-axis approximation. Liu and Tripathi [22] have reported a theoretical framework that accounts for combined effects of laser frequency up-shift, self-focusing, and ring formation by expanding the eikonal and other relevant quantities to the fourth power in r. In a more recent paper [16], they have studied the effect of relativistic mass nonlinearity on self-focusing of a laser pulse in preformed plasmas. In both papers, their treatment is restricted to the singly ionized gases. However, the intensities of laser pulses being used nowadays in experiments are sufficiently high to cause double ionization of the gas, which could adversely affect the laser propagation. Moreover at high intensities, the laser plasma interaction is also relativistic in nature. So, it necessitates developing a theory, which includes the effect of double ionization and relativistic effects simultaneously.

In this paper, we study the relativistic self-focusing of laser pulses and the effect of electron cavitation in a gas undergoing laser-induced double ionization. The intensity is high enough to cause the single ionization almost spontaneously. After a little while, the laser pulse produces double ionization. The inhomogeneity of the electric field along the wavefront of the laser pulse causes more ionization along the propagation axis while less ionization off axis, leading to a density profile exhibiting a strong gradient and with its maximum on the propagation axis. The medium acts like a diverging lens trying to strongly defocus the pulse. However, the ponderomotive force pushes the electrons out of the laser beam and thereby creates a plasma channel, which in turn tries to weaken the ionization-induced divergence of the pulse. When the electron velocity reaches $\upsilon_{osc} = 0.1c$, the relativistic mass nonlinearity starts dominating and after some time, it may take over the ionization induced-divergence so that the pulse self-focuses. We derive the coupled equations governing the behavior of the plasma density and beam width parameter in Section 2. We expand the phase (eikonal) and all other relevant quantities in near-axis approximation. These equations are solved numerically. The results are discussed in Section 3.

2 Coupled equations for plasma density and beam width parameter

Consider the propagation of a laser pulse in a gas jet target. At the entrance into the gas, $z = 0$, the circularly polarized laser field is,

$$\mathbf{E} = (\hat{x} + i\hat{y}) E_0 (r,t)\, e^{-i\omega t},$$
$$E_0^2 = E_{00}^2 \exp\left(-r^2/r_0^2\right) g(t), \quad (1)$$

where $g(t)$ is the temporal shape of the pulse. The rate of tunnel ionization of an atom to the jth state of ionization, in which j electrons have been removed, is given as

$$\Gamma_j = (\pi/2)^{1/2} (I_j/\hbar) \left(\frac{|E\,|}{E_j}\right)^{1/2} \exp\left(-\frac{E_j}{|E\,|}\right), \quad j = 1, 2..., \quad (2)$$

where I_1, I_2... are the ionization potentials for single, double, and higher states of ionization, respectively, $E_j = (4/3)(2m)^{1/2} I_j^{3/2}/e\hbar$ are the characteristic atomic fields, $h = 2\pi\hbar$ is the Planck's constant, $|E\,|$ is the amplitude of the laser field, m is the rest mass of an electron, and e is the magnitude of the electric charge. A similar expression for tunneling rate can also be obtained by using ADK (Ammosov-Delone-Krainov) theory [15]. The ionization of the gas gives rise to a plasma density, n_0, changing in space and time. Let at any instant the densities of singly and doubly ionized ions be n_1 and n_2 respectively. Then $n_0 = n_1 + 2n_2$. Since the ponderomotive force expels electrons radially outward, the electron density distribution gets modified. We define two quantities, $\omega_{p1}^2 = \omega_{p1}'^2 \left(1 - \nabla^2\phi_p/4\pi e n_0\right)$, $\omega_{p2}^2 = \omega_{p2}'^2 \left(1 - \nabla^2\phi_p/4\pi e n_0\right)$ and write

$$\frac{\partial \omega_{p1}^2}{\partial t} = \Gamma_1 \left(\omega_{pm}^2 - \omega_{p1}^2 - \omega_{p2}^2\right) - \Gamma_2 \omega_{p1}^2, \quad (3)$$

$$\frac{\partial \omega_{p2}^2}{\partial t} = \Gamma_2 \omega_{p1}^2, \quad (4)$$

where $\omega_{p1}'^2 = 4\pi n_1 e^2/m$, $\omega_{p2}'^2 = 4\pi n_2 e^2/m$, $\omega_{pm}^2 = 4\pi n_m e^2/m$, n_m is the initial density of neutral atoms, ϕ_p is the ponderomotive potential and Γ_1 and Γ_2 are the ionization rates for single and double ionization, respectively.

Inside the ionizing gas ($z > 0$),

$$\mathbf{E} = (\widehat{x} + i\widehat{y})\, A(t,z,r) \exp(i\phi), \quad (5)$$

where A is the slowly varying complex amplitude (valid when $\partial E/\partial z \ll kE$, $\partial E/\partial t \ll \omega E$, where k is the propagation vector and ω is the frequency of the laser pulse) and $\varphi(t,z)$ is the fast phase of the wave. We define $\omega = \partial\varphi/\partial t$, $k = -\partial\varphi/\partial z$. The laser imparts an oscillatory velocity to electrons

$$\mathbf{v} = \frac{e\mathbf{E}}{mi\omega\gamma}, \quad \gamma = \left(1 + \frac{e^2A^2}{m^2\omega^2c^2}\right)^{1/2}. \quad (6)$$

The laser also exerts a ponderomotive force, $F_p = e\nabla\phi_p$, on the electrons with ponderomotive potential, ϕ_p, as

$$\phi_p = -\frac{mc^2}{e}\left[\left(1 + e^2A^2/m^2\omega^2c^2\right)^{1/2} - 1\right]. \quad (7)$$

Under this force, electrons move radially outward, creating a space charge field $E = -\nabla\phi$. In the quasi-steady state (a time scale longer than an electron plasma period but shorter than an ion plasma period), the net force on the electrons is zero

$$e\nabla(\phi + \phi_p) - \frac{T_e}{n_e}\nabla n_e = 0, \quad (8)$$

where n_e is the modified electron density and T_e is the electron temperature. Equation (8) gives

$$n_e = n_0 \exp\left[e\left(\phi + \phi_p\right)/T_e\right], \tag{9}$$

using equation (9) in the Poisson equation, $\nabla^2\phi = 4\pi e\left(n_e - n_0\right)$, we obtain

$$\phi = -\phi_p + \frac{T_e}{e}\ln\left(1 + \frac{1}{4\pi n_0 e}\nabla^2\phi\right). \tag{10}$$

For $e\phi_p \gg T_e$, one may ignore the second term on the right hand side, hence,

$$\begin{aligned}
&\phi \approx -\phi_p,\\
&n_e = n_0 + \frac{1}{4\pi e}\nabla^2\phi,\\
&\quad = n_0\left[1 - \frac{2c^2}{\omega_p^2 r_0^2}\frac{\gamma^2 - 1}{\gamma}\left(1 - \frac{\gamma^2 + 1}{2\gamma^2}\frac{r^2}{r_0^2}\right)\right],
\end{aligned} \tag{11}$$

n_e is an increasing function of r, having a minimum $n_e = n_0'$ on axis ($r = 0$), where

$$n_0' = n_0\left(1 - \frac{2(\gamma_0^2 - 1)}{\left(\omega_{p0}^2 r_0^2/c^2\right)\gamma_0}\right), \tag{12}$$

where $\gamma_0 = \gamma(r = 0)$, $\omega_{p0}^2 = \omega_p^2\left(t, z, r = 0\right)$. The modified current density of electrons is $\mathbf{J} = -n_e e^2\mathbf{E}/mi\omega\gamma$. Using this modified electron density in the wave equation, we get

$$\nabla^2\mathbf{E} - \frac{1}{c^2}\frac{\partial^2\mathbf{E}}{\partial t^2} = \frac{n_e}{n_0}\frac{\omega_p^2}{\gamma c^2}\mathbf{E}, \tag{13}$$

where $\omega_p^2 = 4\pi n_0\, e^2/m$. Substituting for $\mathbf{E}$, we obtain to successive orders, in the WKB approximation (valid when $\partial E/\partial z \ll kE$)

$$\omega^2 = \frac{n_0'}{n_0}\frac{\omega_{p0}^2}{\gamma_0} + k^2c^2, \tag{14}$$

$$2ik\frac{\partial A}{\partial z} + \frac{2i\omega}{c^2}\frac{\partial A}{\partial t} + \nabla^2{}_\perp A + i\frac{\partial k}{\partial z}A = \frac{1}{c^2}\left(\frac{n_e}{n_0}\frac{\omega_p^2}{\gamma} - \frac{n_0'}{n_0}\frac{\omega_{p0}^2}{\gamma_0}\right)A. \tag{15}$$

In low-density plasma, the fourth term in equation (15) is small. Defining $t' = t - z/c$, $z' = z$ and assuming $\omega_p^2/\omega^2 \ll 1$. Then equation (15) can be written as

$$\frac{2i\omega}{c}\frac{\partial A}{\partial z'} + \nabla_\perp^2 A = \frac{1}{c^2}\left(\frac{n_e}{n_0}\frac{\omega_p^2}{\gamma} - \frac{n_0'}{n_0}\frac{\omega_{p0}^2}{\gamma_0}\right)A. \tag{16}$$

We write $A = A_0\exp\left(iS\right)$, where $A_0\left(t', z', r\right)$ and $S\left(t', z', r\right)$ are real, and separate the real and imaginary parts of equation (16), we get,

$$-\frac{2\omega}{c}\frac{\partial S}{\partial z'}A_0 + \frac{\partial^2 A_0}{\partial r^2} + \frac{1}{r}\frac{\partial A_0}{\partial r} - \left(\frac{\partial S}{\partial r}\right)^2 A_0 = \frac{1}{c^2}\left(\frac{n_e}{n_0}\frac{\omega_p^2}{\gamma} - \frac{n_0'}{n_0}\frac{\omega_{p0}^2}{\gamma_0}\right)A_0, \tag{17}$$

$$\frac{\omega}{c}\frac{\partial A_0^2}{\partial z'} + \left(\frac{\partial^2 S}{\partial r^2} + \frac{1}{r}\frac{\partial S}{\partial r}\right)A_0^2 + \frac{\partial S}{\partial r}\frac{\partial A_0^2}{\partial r} = 0. \tag{18}$$

We expand S, Γ, γ, ω_{pj}^2, as $S = S_0 + S_2 r^2/r_0^2$, $\Gamma_j = \Gamma_{j0} + \Gamma_{j2}r^2/r_0^2$, $\gamma = \gamma_0 + \gamma_2 r^2/r_0^2$, $\omega_{pj}^2 = \omega_{pj0}^2 + \omega_{pj2}^2 r^2/r_0^2$, i.e. in paraxial approximation (valid when $r^2 \ll r_0^2$). In this limit equation (18) can be integrated to give [16]

$$A_0^2 = \frac{E_{00}^2}{f^2}\exp\left(-\frac{r^2}{r_0^2 f^2}\right)g\left(t'\right), \tag{19}$$

where f is the beam width parameter and it is related to S_2 as $S_2 = (1/2f)(\partial f/\partial\xi)$. The parameter ξ is defined as $\xi = z'/R_d$, where $R_d = \omega r_0^2/c$ (twice Rayleigh length). By knowing the value of f, the spot size of the laser beam at any arbitrary point can be estimated as $= r_0 f(\xi)$, where r_0 is the initial spot size of the beam. The condition $f > 1$ stands for the diverging beam where as $f < 1$ stands for the converging beam. The other coefficients involved in the expansions of Γ and γ are

$$\begin{aligned}
&\Gamma_{j0} = \Gamma_{j00}G_j, \quad \Gamma_{j00} = \left(I_j/\hbar\right)\left(\pi/2g_j\right)^{1/2}\exp\left(-g_j\right),\\
&g_j = E_j/E_{00}, \quad G_j = \exp\left(g_j - g_{j1}\right)/f^{1/2},\\
&g_{j1} = g_j f, \quad \Gamma_{j2} = -\left(1 + 2g_{j1}\right)\Gamma_{j0}/4f^2,\\
&\gamma_0 = \left(1 + e^2E_{00}^2 g(t')/m^2\omega^2c^2f^2\right)^{1/2},\\
&\gamma_2 = -e^2E_{00}^2 g(t')/2m^2\omega^2c^2\gamma_0 f^4.
\end{aligned}$$

$j = 1$ and 2 refer to single and double ionization respectively. Introducing dimensionless quantities $\upsilon_0/c = eE_{00}/m\omega c$, $T = \Gamma t'$, $\Gamma = (I_1/\hbar)(\pi/2)^{1/2}$ and collecting the coefficients of various powers of r in equations (3), (4) and in equation (17), we obtain

$$\frac{\partial\omega_{p10}^2}{\partial T} = \exp(-g_1 f)\left(\omega_{pm}^2 - \omega_{p10}^2 - \omega_{p20}^2\right)/\left(g_1 f\right)^{1/2} - 1.22\exp\left(-3.29g_1 f\right)\omega_{p10}^2/\left(g_1 f\right)^{1/2}, \tag{20}$$

$$\begin{aligned}
\frac{\partial\omega_{p12}^2}{\partial T} = &-\frac{\left(1 + 2g_{11}\right)}{4f^{5/2}g_1^{1/2}}\exp\left(-g_1 f\right)\left(\omega_{pm}^2 - \omega_{p10}^2 - \omega_{p20}^2\right)\\
&-\frac{\exp\left(-g_1 f\right)}{\left(g_1 f\right)^{1/2}}\left(\omega_{p12}^2 + \omega_{p22}^2\right)\\
&+1.22\frac{\left(1 + 6.58g_{11}\right)}{4f^{5/2}g_1^{1/2}}\exp(-3.29g_1 f)\omega_{p10}^2\\
&-1.22\frac{\exp\left(-3.29g_1 f\right)}{\left(g_1 f\right)^{1/2}}\omega_{p12}^2,
\end{aligned} \tag{21}$$

$$\frac{\partial \omega_{p20}^2}{\partial T} = 1.22 \frac{\exp\left(-3.29 g_1 f\right)}{\left(g_1 f\right)^{1/2}} \omega_{p10}^2, \tag{22}$$

$$\frac{\partial \omega_{p22}^2}{\partial T} = -1.22 \frac{\left(1 + 6.58 g_{11}\right)}{4 f^{5/2} g_1^{1/2}} \exp\left(-3.29 g_1 f\right) \omega_{p10}^2 + 1.22 \frac{\exp\left(-3.29 g_1 f\right)}{\left(g_1 f\right)^{1/2}} \omega_{p12}^2, \tag{23}$$

$$\frac{d^2 f}{d\xi^2} = \frac{1}{f^3} - \frac{\left(\omega_{p12}^2 + 2\omega_{p22}^2\right) r_0^2 f}{\gamma_0 c^2} - \frac{r_0^2 \left(\omega_{p10}^2 + 2\omega_{p20}^2\right) v_0^2 g\left(t'\right)}{2 c^4 \gamma_0^3 f^3} - f\left(1 - \frac{1}{\gamma_0^4}\right) - \frac{2 v_0^2 g\left(t'\right)}{c^2 \gamma_0^4 f^3}. \tag{24}$$

The boundary conditions at $\xi = 0$ are: $f = 1$, $\partial f / \partial \xi = 0$, and $S_0 = 0$. The first two terms on the right hand side of equation (24) represent divergence due to diffraction and nonlinear refraction, the third term gives the relativistic self-focusing, whereas the last two terms include the effect of electron cavitation. In the absence of the last three terms the laser pulse would continue to diverge. However, when the first two terms exactly balance the last three terms, the pulse propagates without any divergence. We choose $g(t') = \tanh\left(t'/\tau\right)$ for $t' > 0$ and zero otherwise, where τ is the pulse rise time.

We have solved these equations numerically and plotted the beam width parameter, f, as a function of ξ, at different times, for different laser powers. Figure 1a shows the variation of beam width parameter, f, with ξ for $\Omega_{pm}^2 \equiv \omega_{pm}^2/\omega^2 = 0.03$. The other parameters are $g_1 = 0.4$ corresponding to $I_1 = 24$ eV, first ionization potential of helium, laser intensity $I_L \approx 6 \times 10^{17}$ W/cm^2, $\tau = 50$ fs. The foot of the pulse ($T = 50$ corresponding to 1 fs) causes single ionization of the gas, which produces sharp electron density gradient, resulting in a strong defocusing of the pulse. Later in time ($T = 200$ corresponding to 4 fs), the pulse produces double ionization of the gas. It results in the formation of a very strong radial density gradient, hence severe defocusing of the laser pulse. Later on ($T = 500$ corresponding to 10 fs), the density profile flattens and the relativistic mass nonlinearity together with electron cavitation self-focuses the laser pulse. At a higher gas pressure, the front part of the pulse faces more divergence while the later part of the pulse self-focuses earlier in time (cf. Fig. 1b). At a higher laser intensity $I_L \approx 4 \times 10^{18}$ W/cm^2 (Fig. 2), the laser pulse produces single as well as double ionization rapidly (the effect of double ionization appears as early as $T = 50$). Due to this, the electron density profile tends to flatten rather quickly, resulting in less defocusing of later part of the pulse ($T = 100$) as compared to the previous case. At larger times ($T = 200$ corresponding to 6 fs), the relativistic mass nonlinearity and electron cavitation self-focuses the laser pulse. At higher gas pressure (Fig. 2b), similar type of behavior can be noted as in Figure 1b. We have also plotted the beam width parameter, f, as a function of ξ, at different times in a case when only single ionization is present in the system (Figs. 3 and 4). A comparison of Figure 1 with Figure 3 shows that at the foot of the pulse divergence solely comes from the density gradient caused by the single ionization of the gas. At larger times ($T = 200$, Fig. 1), double ionization of the gas occurs, which causes severe divergence of the pulse, which is completely absent in Figure 3. However at larger times ($T = 500$, Fig. 3a), the density profile flattens and the relativistic mass nonlinearity and electron cavitation start dominating ionization-induced divergence, the laser pulse propagates without any significant divergence. A similar

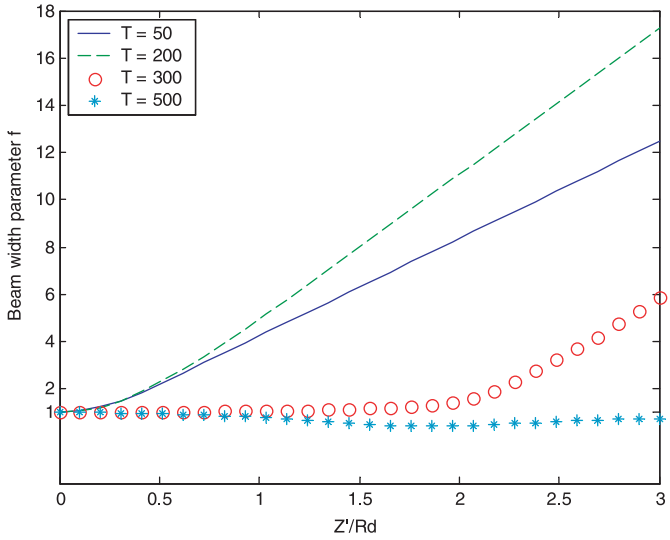

(a)

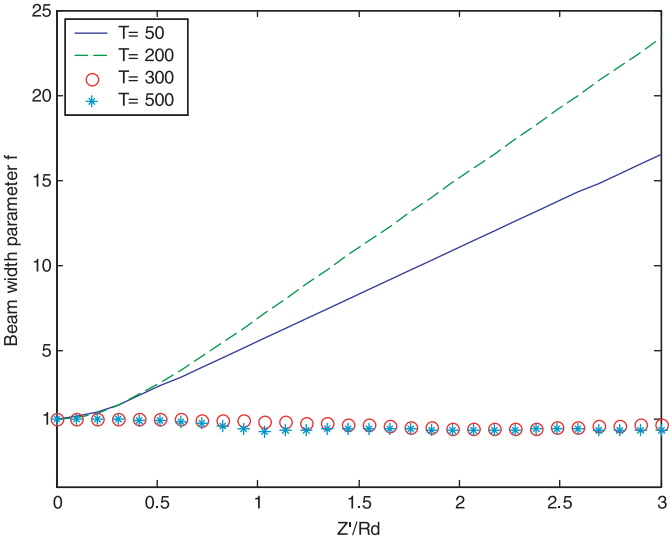

(b)

Fig. 1. Variation of beam width parameter, f, at different retarded times T, with ξ at a laser intensity $I_L = 6 \times 10^{17}$ W/cm^2 and $v_0^2/c^2 = 0.5$ (a) for an electron density $\Omega_{pm}^2 = 0.03$ (b) for an electron density $\Omega_{pm}^2 = 0.05$. The other parameters are, $\omega r_0/c = 20$, $\tau = 50$ fs and $g_1 = 0.4$ corresponding to the laser intensity.

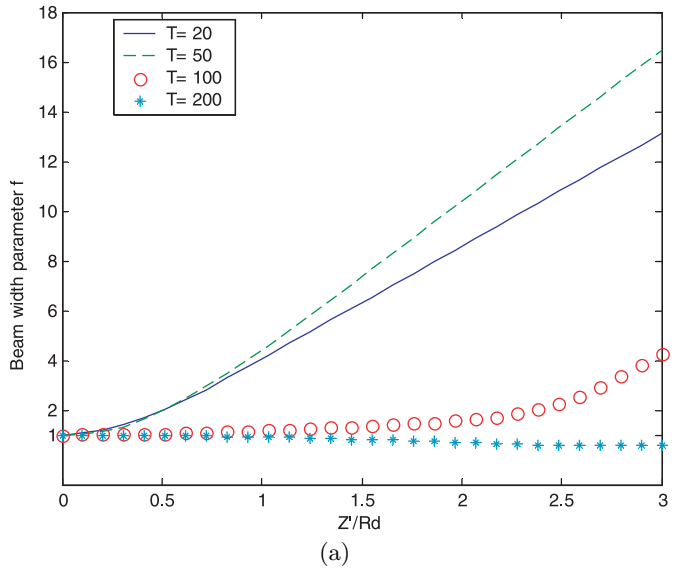

(a)

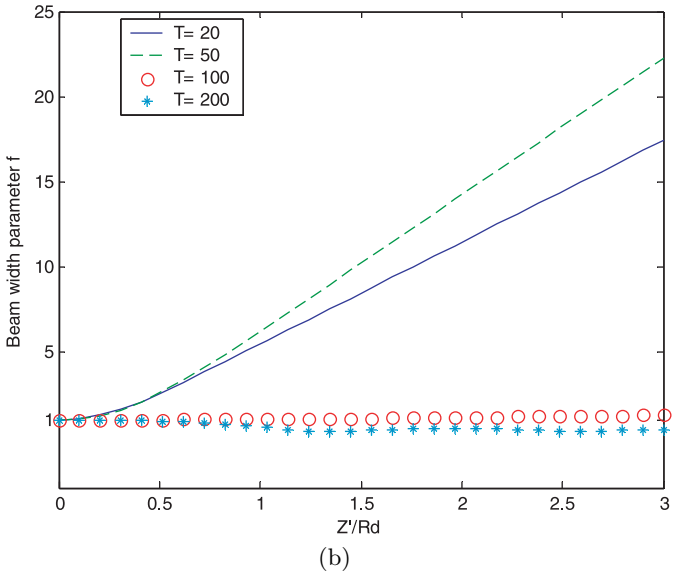

(b)

Fig. 2. Variation of beam width parameter, f, at different retarded times T, with ξ at a laser intensity $I_L = 4\times10^{18}$ W/cm^2, $v_0^2/c^2 = 1.5$ and $g_1 = 0.14$ corresponding to the laser intensity (a) for an electron density $\Omega_{pm}^2 = 0.03$ (b) for an electron density $\Omega_{pm}^2 = 0.05$. The other parameters are the same as in Figure 1.

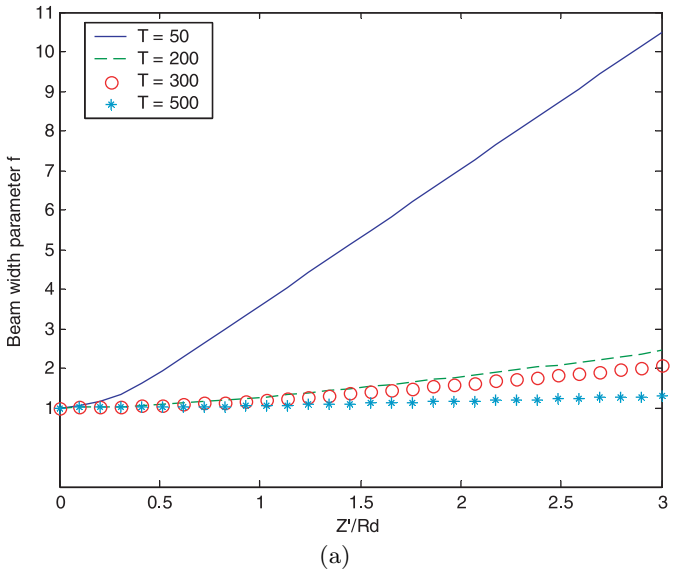

(a)

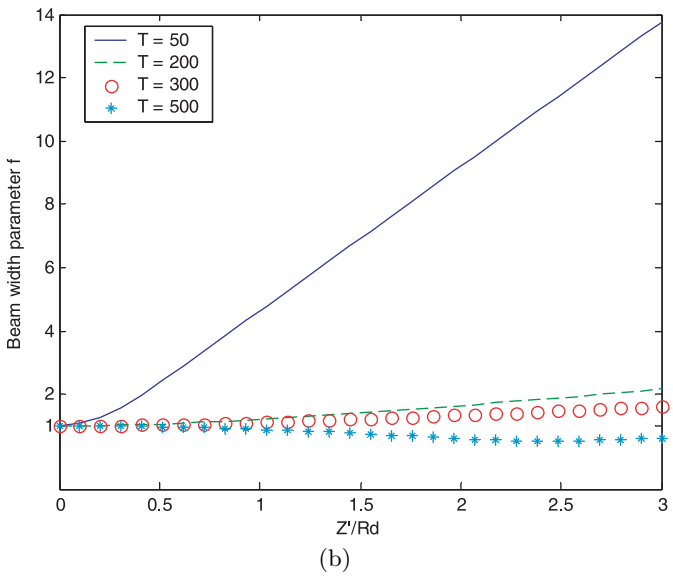

(b)

Fig. 3. Variation of beam width parameter, f, at different retarded times T, with ξ in a case when only single ionization is present in the system at a laser intensity $I_L = 6\times10^{17}$ W/cm^2, (a) for an electron density $\Omega_{pm}^2 = 0.03$ (b) for an electron density $\Omega_{pm}^2 = 0.05$. The other parameters are the same as in Figure 1.

3 Discussion

behavior can also be observed at higher laser intensity (cf. Fig. 4a). At a higher gas pressure, the later part of the pulse ($T = 300$, 500 in Fig. 1b) self-focuses. However in the case of single ionization (Fig. 3b), the part corresponding to $T = 300$ still faces mild divergence. Since double ionization produces twice as much electron density as single ionization. The last three terms in equation (24) start dominating over first two terms very early resulting in self-focusing of the pulse at lower times. The same type of behavior can also be noted at higher laser intensity (cf. Figs. 2b and 4b).

A fast rising flattop Gaussian laser pulse with peak intensity $I_L \geq 10^{17}$ W/cm^2, produces single ionization of the He gas rapidly. At the foot of the pulse, single ionization produces a sharp electron density profile resulting in strong defocusing of the pulse. As the intensity of the pulse rises, single ionization saturates but double ionization causes strong radial density gradient and severe defocusing of the pulse. On a longer time scale, $t' = 500\Gamma^{-1}$ (of the order of a few laser periods), when double ionization saturates in the axial region and acquires a substantial level in the non-axial

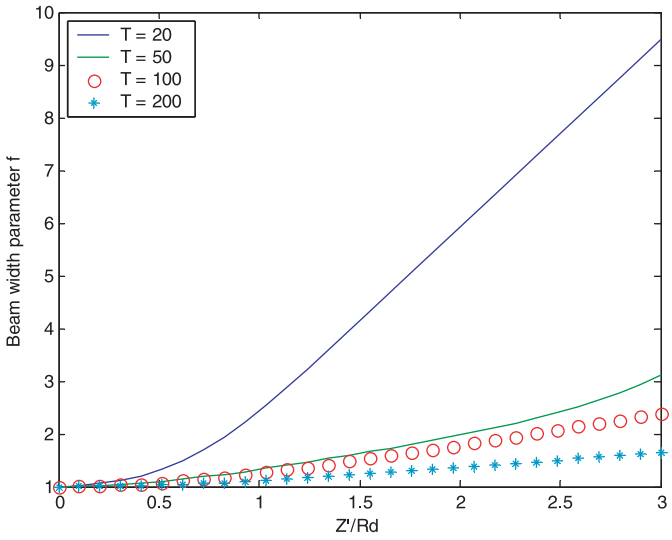

(a)

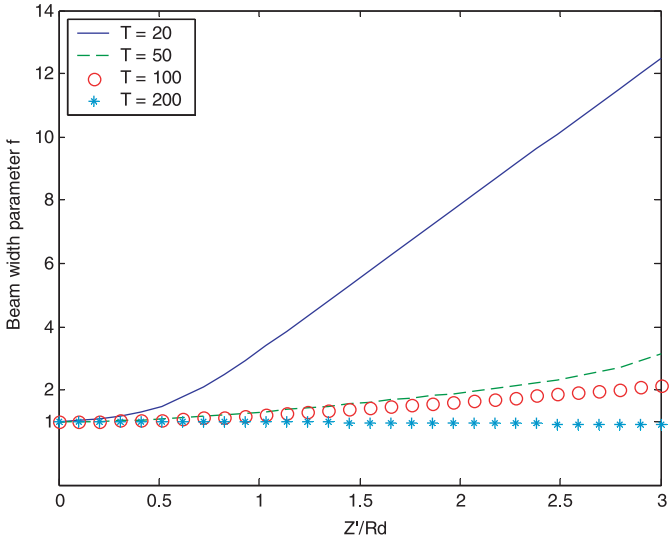

(b)

Fig. 4. Variation of beam width parameter, f, at different retarded times T, with ξ in a case when only single ionization is present in the system at a laser intensity $I_L = 4 \times 10^{18}$ W/cm^2 (a) for an electron density $\Omega_{pm}^2 = 0.03$ (b) for an electron density $\Omega_{pm}^2 = 0.05$. The other parameters are the same as in Figure 1.

regions, the relativistic mass nonlinearity along with electron cavitation dominates the ionization induced divergence and the pulse self-focuses. At a higher intensity of $I_L \approx 10^{18}$ W/cm^2, the laser pulse produces single as well as double ionization of the gas very quickly, due to which defocusing and flattening of the density profile take place in a short period of time. Thereafter the relativistic mass nonlinearity and electron cavitation dominate the ionization-induced divergence and the pulse self-focuses. At a higher gas pressure, the relativistic mass nonlinearity and electron cavitation dominate ionization-induced divergence very early resulting in the self-focusing of the laser pulse at lower time. In this paper we have not assumed the axial inhomogeneity in gas jet profile. However, if it exists then the various ω_{pj}^2 in equation (24) would be a function of z' resulting in different rates of defocusing and focusing during the course of the propagation. The present treatment is valid in paraxial ray approximation.

References

1. D. Umstadter, J. Phys. D: Appl. Phys. **36**, R151 (2003)
2. M. Honda, J. Meyer-ter-Vehn, A. Pukhov, Phys. Plasmas **7**, 1302 (2000)
3. K.A. Tanka et al., Phys. Plasmas **7**, 2014 (2000)
4. G.D. Tsakiris, C. Gahn, V.K. Tripathi, Phys. Plasmas **7**, 3017 (2000)
5. C.S. Liu, V.K. Tripathi, *Interaction of Electromagnetic waves with Electron beams and Plasmas* (World Scientific, Singapore, 1994), Chap. 4
6. G. Malka, E. Lefebvre, J.E. Miquel, Phys. Rev. Lett. **78**, 3314 (1997)
7. D.L. Bruhwiler, P.A. Dimitrov, J.R. Cary, E. Esarey, W. Leemans, R.E. Giacone, Phys. Plasmas **10**, 2022 (2003)
8. C. Gahn, G.D. Tsakiris, A. Pukhov, J. Meyer-ter-Vehn, G. Pretzler, P. Thirolf, D. Habs, K.J. Witte, Phys. Rev. Lett. **83**, 4772 (1999)
9. S. Dobosz, P. D'Oliveira, S. Hulin, P. Monot, F. Reau, T. Auguste, Phys. Rev. E **65**, 047403 (2002)
10. A. Ting, K. Krushelnick, H.R. Burris, A. Fisher, C. Manka, C.J. Moore, Opt. Lett. **21**, 1096 (1996)
11. P. Sprangle, E. Esarey, J. Krall, Phys. Rev. E **54**, 4211 (1996)
12. A. Maksimchuk, S. Gu, K. Flippo, D. Umstadter, Phys. Rev. Lett. **84**, 4108 (2000)
13. G.S. Sarkisov, V.Yu. Bychenkov, V.T. Tikhonchuk, A. Maksimchuk, S.Y. Chen, R. Wagner, G. Mourou, D. Umstadter, JETP Lett. **66**, 828 (1997)
14. L.V. Keldysh, Sov. Phys. JETP **20**, 1307 (1965)
15. M.V. Ammosov, N.B. Delone, V.P. Krainov, Sov. Phys. JETP **64**, 1191 (1986)
16. C.S. Liu, V.K. Tripathi, J. Opt. Soc. Am. A **18**, 1714 (2001)
17. A. Borisov et al., Phys. Rev. Lett. **68**, 2309 (1992)
18. P. Chessa, E. De Wispelaere, F. Dorchies, V. Malka, J.R. Marques, G. Hamoniaux, P. Mora, F. Amiranoff, Phys. Rev. Lett. **82**, 552 (1999)
19. R. Fedosejevs, X.F. Wang, G.D. Tsakiris, Phys. Rev. E **56**, 4615 (1997)
20. G.S. Sarkisov, V.Yu. Bychenkov, V.N. Novikov, V.T. Tikhonchuk, A. Maksimchuk, S.Y. Chen, R. Waner, G. Mourou, D. Umstadter, Phys. Rev. E **59**, 7042 (1999)
21. E. Esarey, P. Sprangle, J. Krall, IEEE J. Quant. Electron. **33**, 1879 (1997)
22. C.S. Liu, V.K. Tripathi, Phys. Plasmas **7**, 4360 (2000)